

KA-TP-19-1999
hep-ph/9911452
November 1999

Radiative corrections to pair production of charged Higgs bosons at TESLA¹

Jaume Guasch, Wolfgang Hollik, Arnd Kraft
*Institut für Theoretische Physik, Universität Karlsruhe,
D-76128 Karlsruhe, Germany*

ABSTRACT

Charged Higgs particles are a common feature of many extensions of the Standard Model. While its existence with masses up to the TeV scale can be probed at the Tevatron Run II and LHC hadron colliders, a precise determination of its properties would have to wait for a high energy e^+e^- linear collider. We have computed the complete one-loop electroweak corrections to the cross-section for charged Higgs bosons pair production in e^+e^- collisions, in the framework of general Two Higgs Doublet Models, as well as the Minimal Supersymmetric Standard Model. A study is presented for typical values of the model parameters, showing the general behaviour of the corrections.

¹Talk presented by J. Guasch at the Vth workshop in the 2nd ECFA/DESY Study on Physics and Detectors for a Linear Electron-Positron Collider, Obernai (France) 16-19th October, 1999.

1 Introduction

During the next decades the Tevatron and LHC hadron colliders will explore the TeV energy region, performing tests of the Standard Model (SM) at energies higher than ever before and searching for new physics phenomena. While these machines are well suited to discover possible new particles with large masses (e.g. up to 2.5 TeV for the LHC [1]), the next generation of high energy and high luminosity e^+e^- linear colliders, such as TESLA, are the best environment to make a precise determination of their properties. One of the major goals of TESLA will be to perform precision measurements of the properties of heavy particles, like the top quark, reaching a level comparable to the LEP I determination of the Z boson observables. In view of these prospects it is necessary to account for radiative corrections in order to have theoretical predictions with an uncertainty smaller than the experimental one. In the case of processes involving non-standard particles, precision studies are a crucial requirement for their accurate identification within the various conceivable extensions of the SM.

A common feature of many SM extensions is the augmentation of the Higgs sector, predicting the presence of additional neutral Higgs bosons and of charged Higgs particles, which are in the focus of this study. The simplest SM extension, the so-called Two Higgs Doublet Model (2HDM) [2], includes an additional Higgs doublet in the scalar sector. From a theoretical point of view, the supersymmetric (SUSY) extensions of the SM are more appealing; the simplest version in this class of models is the Minimal Supersymmetric Standard Model (MSSM) [3].

In the MSSM, the Higgs sector is determined at the tree-level by just two parameters, which are conventionally chosen to be the ratio of the two vacuum expectation values, $\tan\beta = v_2/v_1$, and a mass which we take as the charged Higgs mass M_{H^\pm} . The relations between the various masses, however, get significant corrections at higher orders [4].

In the general 2HDM, all the masses and the mixing angle α for the CP-even neutral Higgs bosons are independent parameters [2]; in addition we have an independent parameter which enters the Higgs bosons self-couplings, which we take to be λ_5 in the convention of [2]. Indirect constraints on charged Higgs bosons are obtained from present low energy data on the branching ratio $BR(b \rightarrow s\gamma)$ which does not favour low values of the charged Higgs mass in the 2HDM of type II [5]; the latest analysis indicates a value for M_{H^\pm} higher than 165 GeV [6].

If the charged Higgs particle is light enough, it will be pair-produced at TESLA at appreciable rates. The detailed discussion of the production cross-section on the basis of a complete one-loop calculation in the general 2HDM and the MSSM, incorporating also soft and hard photon bremsstrahlung, is the content of this article.

The first question to be addressed is the relevance of studying charged Higgs pair production. In Fig. 1 we have displayed the tree-level cross-section $\sigma^{(0)}(e^+e^- \rightarrow H^+H^-)$ as a function of the charged Higgs mass for different values of the center of mass energy \sqrt{S} . The typical value of this cross-section lies in the ballpark of several fb, unless the center of mass energy is very close to the production threshold.

For definiteness, we will concentrate our discussion in this article on two scenarios: the

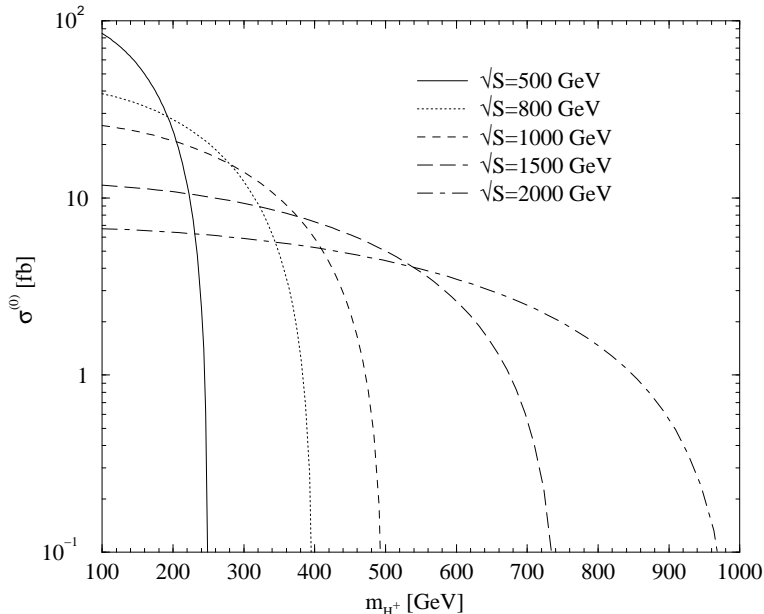


Figure 1: Lowest order cross-section for the process $e^+e^- \rightarrow H^+H^-$ as a function of the charged Higgs boson mass, for different values of the center of mass energy \sqrt{S} .

first one with an energy of $\sqrt{S} = 500$ GeV and a charged Higgs of $M_{H^\pm} = 220$ GeV (set A), the second one with a higher energy of $\sqrt{S} = 800$ GeV and a charged Higgs mass of $M_{H^\pm} = 300$ GeV (set B). A high luminosity of $500 \text{ fb}^{-1}/\text{year}$ for the TESLA collider is assumed. Under these conditions $\sigma^{(0)}(H^+H^-) = 11.8 \text{ fb}$ [12.3 fb] for set A [B] is obtained, which means the production of ca. 5900 [6150] pairs of charged Higgs particles per year. For set B a recent study [7] shows that the background to this process can be reduced very efficiently, maintaining most of the signal events and allowing for a precise determination of the mass of the charged Higgs particle.

There are also other processes where a charged Higgs boson could be produced at TESLA. The associated production $e^+e^- \rightarrow H^\pm W^\mp$ [8] is one-loop mediated in lowest order, and thus its cross-section is smaller than that of H^+H^- pair production, provided the latter channel is open. There exists also the associated production with quarks of the third generation $H^+\bar{t}b$, which suffers of being a three-body production; but it could be important in certain regions of the parameter space. Finally, if the charged Higgs is light enough, it could arise from primary top quarks decaying according to $t \rightarrow H^+b$. The non-SM radiative corrections to this process have been studied, and are found to be very large, with important consequences for the charged Higgs search in the region $M_{H^\pm} < m_t$ [9].

The second question to be addressed is the size of the radiative corrections to $e^+e^- \rightarrow H^+H^-$. They can be expected to be important because of the potentially large couplings associated with the Higgs sector, to wit: the Yukawa coupling of the top quark, and of the bottom quark at large $\tan\beta$ for the type II 2HDM; the couplings involving squarks of the

third generation in the MSSM; and the self-couplings of the Higgs particles in the general 2HDM.

The third question to be addressed is the possibility to discriminate between the different models by means of precise measurements of the cross-section. This point is closely related to the previous one, since the detailed structure of the model enters only at the quantum level, through the radiative corrections.

In this note we will restrict ourselves to the presentation of the main results of the one-loop calculation; the complete expressions and a comprehensive analysis will be presented elsewhere [10]. The computation has been thoroughly checked, invoking also a numerical check versus a code generated by the computer-algebra system *FeynArts* and *FormCalc* [11]. The one-loop corrections for this process were also discussed in Ref. [12] for the fermion and sfermion contributions, and in Refs. [13, 14] for the Higgs, gauge and fermion sector in the case of the 2HDM of type II and also of the MSSM Higgs sector. Our results are in good agreement with those of Ref. [14]. In the present work we have also computed the corrections for the case of the type I 2HDM and the contributions from the chargino-neutralino sector in the MSSM. Moreover, we present an analysis of the forward-backward asymmetry, including also the complete $O(\alpha)$ QED corrections with hard photons.

2 One-loop corrections to $\sigma(e^+e^- \rightarrow H^+H^-)$

The lowest-order differential cross-section for $e^+e^- \rightarrow H^+H^-$ is determined exclusively by the gauge couplings and by the mass M_{H^\pm} , which enters only the phase space. Moreover, the angular distribution is symmetric in the production angle θ . Through the loop contributions, the cross-section becomes dependent on the details of the Higgs sector and, in addition, of the SUSY particles in the case of a supersymmetric model. Specifically, also an angular asymmetry is induced, giving rise to a forward-backward or charge asymmetry.

2.1 QED corrections

As often done in the discussion of one-loop corrections, we first separate the subclass of the QED (photonic) corrections. The contributions of this class are universal in the sense that they only depend on the charge of the particles but not on the details of the underlying model. They are in general numerically important, and it is necessary to have them under control if one wants to observe the small effects resulting from the residual non-QED one-loop contributions with their model-specific informations.

We have computed the complete $O(\alpha)$ QED corrections, which arise from the exchange of virtual photons and from real photon bremsstrahlung. Both the soft and the hard photon emission are included. The bulk of the QED corrections is given by initial state radiation (ISR), which lowers the effective center-of-mass energy available for the annihilation process. These corrections are typically quite large; one therefore has to take into account also

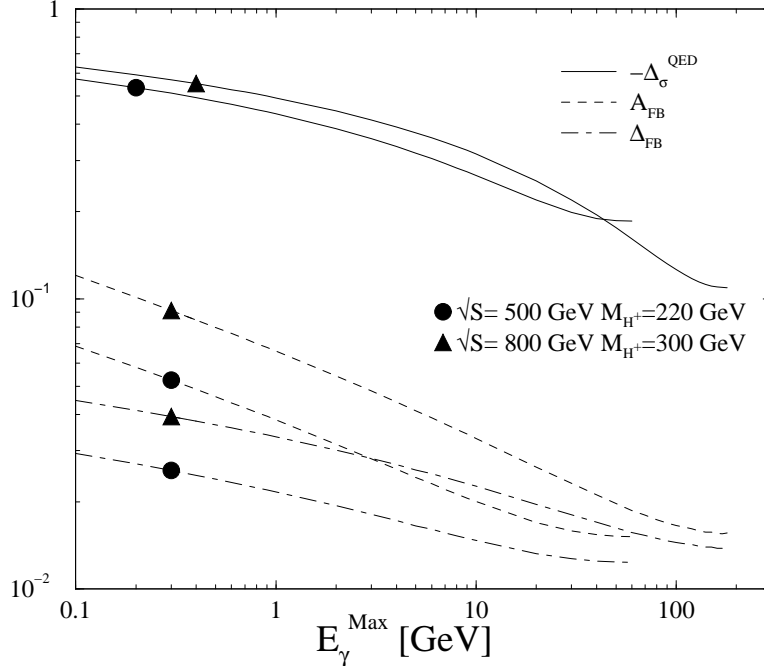


Figure 2: Photonic (QED) corrections to the total cross-section $\sigma(e^+e^- \rightarrow H^+H^-)$ (with reversed sign) and the forward-backward asymmetry as a function of the photon energy cutoff.

higher orders with a resummation of leading terms. For our calculation we have used the resummed leading ISR corrections as given by the structure function method (see e.g. [15]).

The interference between initial and final state radiation is of special interest since it is responsible, together with the box diagrams containing at least one virtual photon, for a QED-induced charge asymmetry, which has to be well separated from the charge asymmetry caused by the model-specific non-QED box diagrams.

In Fig. 2 we display the QED corrections to the integrated cross-section (with reversed sign) as well as the QED contributions to the forward-backward asymmetry A_{FB} and to the quantity Δ_{FB} in eq. (3), as a function of the cut-off to the photon energy assuming that photons with energy $E \leq E_\gamma^{Max}$ are not resolved. The relative correction Δ_σ is defined in the following way

$$\sigma = \sigma^{(0)} + \delta\sigma = \sigma^{(0)}(1 + \Delta_\sigma) , \quad (1)$$

where σ is the integrated cross-section including radiative corrections and $\sigma^{(0)}$ is the tree-level prediction. We see that for a more inclusive cross-section, allowing for photons with higher energies, the QED corrections decrease. For the choice of parameters as in Fig. 2 the QED corrections to the total cross-section are negative, ranging from -60% to -20% [-10%] for set A [B]. The asymmetry is discussed in section 3.

2.2 Weak Corrections

The weak corrections form the complementary subclass of the non-QED one-loop contributions, with model-specific information beyond that in the tree-level amplitude. In Figs. 3-5 we present a summary of the numerical results found for the pure weak corrections, pointing out their typical behaviour. For the interpretation of the analysis it is useful to separate the different contributions arising from the various particles in the loops, as well as to distinguish between initial state (IS) corrections (the e^+e^- vertex corrections), final state (FS) corrections (the H^+H^- vertex corrections), self-energies of the intermediate photon and Z boson, and box diagrams where two internal lines connect the external e^+e^- legs to the external H^+H^- legs. One should keep in mind, however, that for loops with gauge bosons the separation between the different topologies is in general gauge dependent.

We classify the weak corrections as follows:

- The first set of diagrams is formed by loops which contain gauge bosons, together with electrons, neutrinos, and Higgs particles. These particles contribute to the IS, FS, self-energies, and box corrections. Their contributions are sizeable (see below), and they are specially interesting in the parameter range of $\tan \beta = 2 - 20$.
- Vertex one-loop diagrams with Higgs boson exchange only contribute to the FS corrections; in the IS they are negligible. In these kind of diagrams the potentially large Higgs self-couplings occur in the general 2HDM, whereas in the MSSM the Higgs self-couplings are always small.
- The loops with top and bottom quarks contribute to the FS corrections through the Yukawa couplings, which are given by [2]

$$\lambda_t \equiv \frac{m_t}{v_2} \sim \frac{m_t}{\sin \beta} \quad , \quad \lambda_b^{\{I, II\}} \equiv \frac{m_b}{\{v_2, v_1\}} \sim \frac{m_b}{\{\sin \beta, \cos \beta\}} \quad , \quad (2)$$

where the expression for λ_b depends on the type of the 2HDM. We see that these couplings can be important either at low and (for the type II 2HDM) large values of $\tan \beta$. In the MSSM, only type II is realized.

- In the MSSM we have in addition the corrections due to squarks, with the most important ones from the third generation squarks (\tilde{t}, \tilde{b}). In this case not only the Yukawa-type couplings (2) are large, but also the trilinear squark-squark-Higgs boson couplings can be quite huge, leading to large corrections.
- Finally we have the diagrams with loops containing all the plethora of chargino, neutralino, and selectron-sneutrino. These particles contribute to all kind of topologies. As we have found, their contribution to the total cross-section is generally rather small, at the level of a few per mille; however, they do contribute to the forward-backward asymmetry.

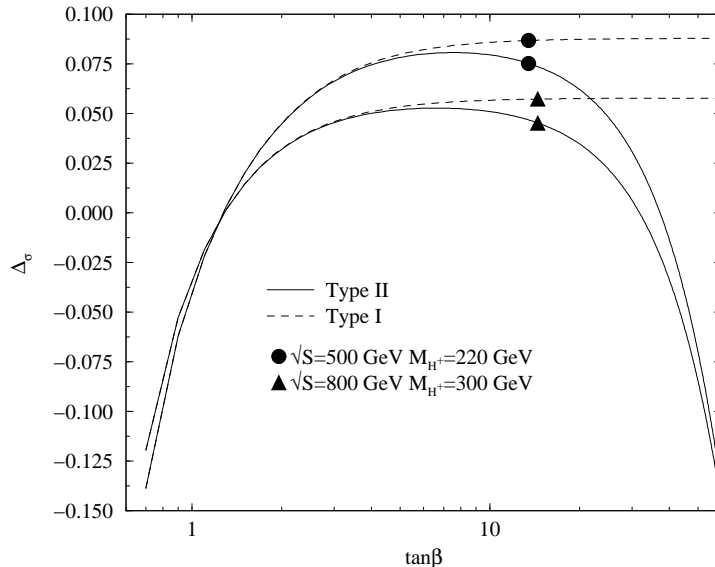


Figure 3: One-loop weak radiative corrections to $\sigma(e^+e^- \rightarrow H^+H^-)$ for the 2HDM of type I and II as a function of $\tan\beta$. The other parameters are: $M_{h^0} = 150$ GeV, $M_{H^0} = 500$ GeV, $M_{A^0} = M_{H^\pm} - 20$ GeV, the scalar mixing angle $\alpha = \pi/2 - \beta$, and the parameter $\lambda_5 = 2\pi\alpha_{em}M_{H^0}^2/(\sin^2\theta_W M_W^2)$.

We start our numerical analysis with the case of the general 2HDM. In Fig. 3 we present the evolution of the corrections with $\tan\beta$ for fixed typical values of the other parameters. It should be stated that in all our numerical analysis we have respected present constraints on the parameter space, taking care that the additional contributions to the ρ parameter do not surpass present experimental errors.

The free parameter λ_5 in the Higgs bosons self-couplings is a general feature of the unconstrained 2HDM. For $0.7 < \tan\beta < 2$ it modifies the cross-section not more than $\pm 10\%$, even for rather large values $\lambda_5 < 20$. For large $\tan\beta$, however, λ_5 enters the loop diagrams in the combination $\sim \lambda_5 \tan\beta$. This gives rise to large positive corrections, which would be in conflict with perturbative consistency if we let λ_5 vary freely. In the following we restrict our discussion to small values of λ_5 .

From Fig. 3 we can see that for low $\tan\beta$ values both of the 2HDMs give the same predictions. In this region the radiative corrections are dominated by the top quark Yukawa coupling (2) and can amount to -15% . The size of the corrections decreases with the top quark Yukawa coupling, and a flat region exists for the intermediate range of $\tan\beta = 2-10$. In this region the radiative corrections are driven by the gauge- and Higgs self-couplings. For our chosen set of parameters they amount to a $\sim 7\%$ positive correction. For larger energies or lower charged Higgs boson masses the corrections can be slightly negative [10]. For the type II 2HDM at large $\tan\beta$, the bottom quark Yukawa coupling (2) enters the game, driving again towards negative corrections for large $\tan\beta$. For the type I 2HDM, on

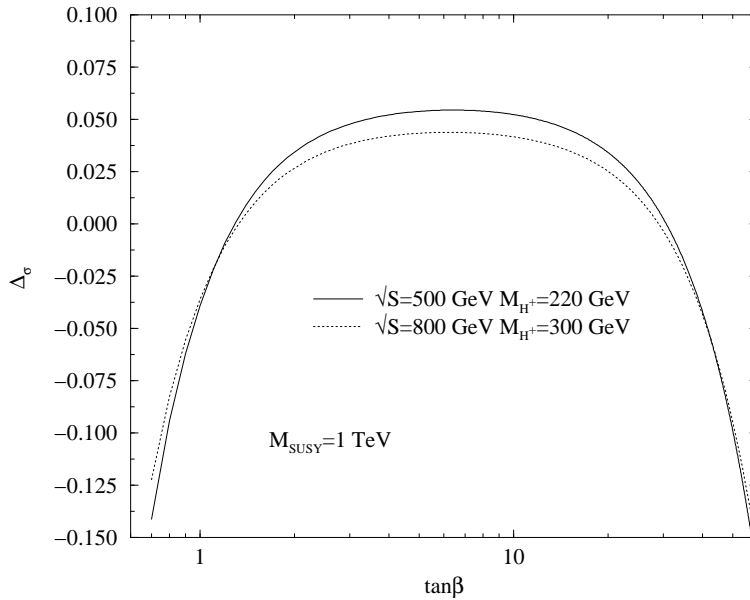


Figure 4: One-loop weak corrections to $\sigma(e^+e^- \rightarrow H^+H^-)$ for the MSSM as a function of $\tan\beta$. The SUSY parameters are taken to be $\mu = m_{\tilde{q}_L} = m_{\tilde{q}_R} = A_q = M_1 = M_2 = 1$ TeV.

the other hand, the corrections reach an asymptotic value.

In Fig. 4 we have plotted the weak corrections for the case of the MSSM, assuming a SUSY mass spectrum in the ballpark of 1 TeV. The corrections show a behaviour similar to that of a type II 2HDM. If the SUSY spectrum is lighter, however, the situation changes. Fig. 5 shows the corrections as a function of the sbottom mass parameter, for different choices of the mixing parameters. Indeed, when the squark masses get low enough ($m_{\tilde{q}} \lesssim 500$ GeV) they give positive contributions to the corrections, which can be sizeable even when they are too heavy to be directly produced at TESLA. Lighter squark masses can make the corrections negative, thereby yielding much larger values than the 2HDM case for the same value of $\tan\beta$. This is the only potentially large loop effect from SUSY particles, since the contributions from the chargino-neutralino sector are comparatively tiny (below the 1% level).

3 The forward-backward asymmetry

In principle the forward-backward asymmetry seems to be an appropriate observable for testing the type of electroweak model for the charged Higgs bosons. In the case of the MSSM there are much more box-type diagrams (with virtual charginos and neutralinos) that contribute to the asymmetry, and one might expect that, although their effect on the total cross-section is negligible, they could amount to an observable contribution to the asymmetry.

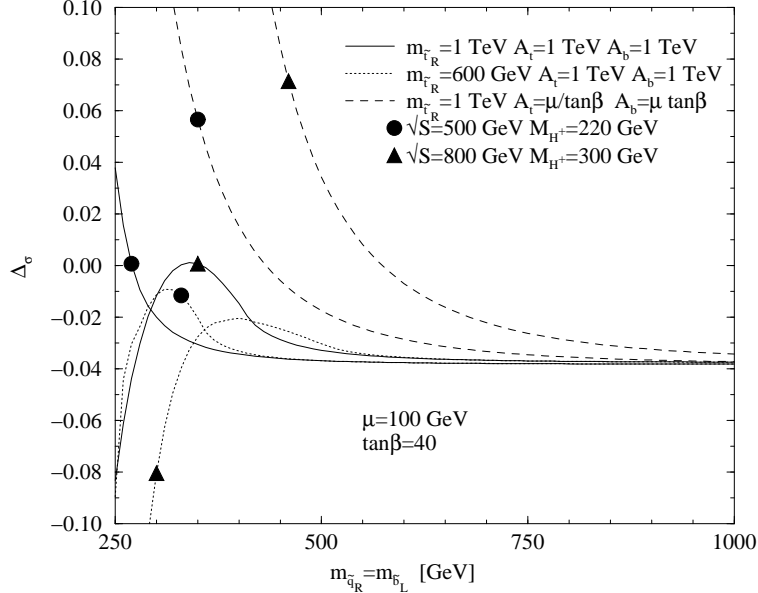


Figure 5: One-loop weak corrections to $\sigma(e^+e^- \rightarrow H^+H^-)$ in the MSSM as a function of the bottom squark mass parameter. The other parameters are given in the frame.

The forward-backward asymmetry is defined as

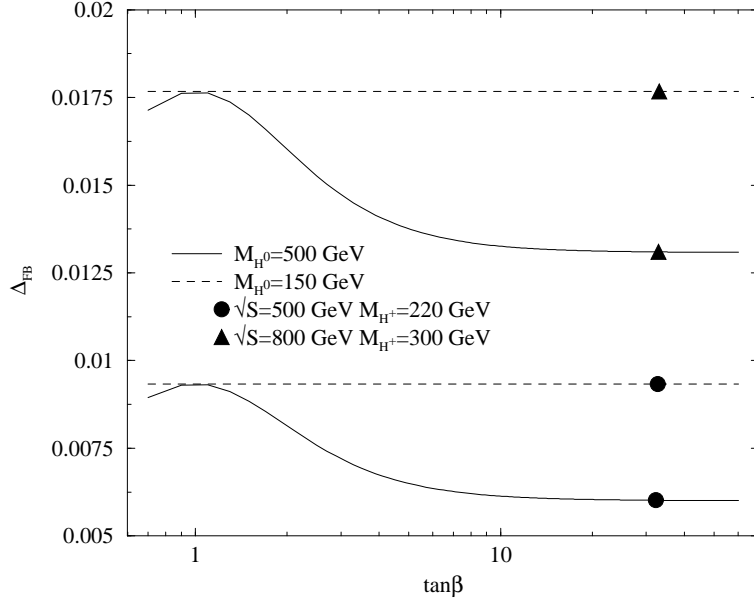
$$A_{FB} = \frac{\sigma^F - \sigma^B}{\sigma} = \Delta_{FB} \frac{1}{1 + \Delta_\sigma} . \quad (3)$$

Δ_{FB} denotes the antisymmetric part of the cross-section normalized to the tree-level cross-section,

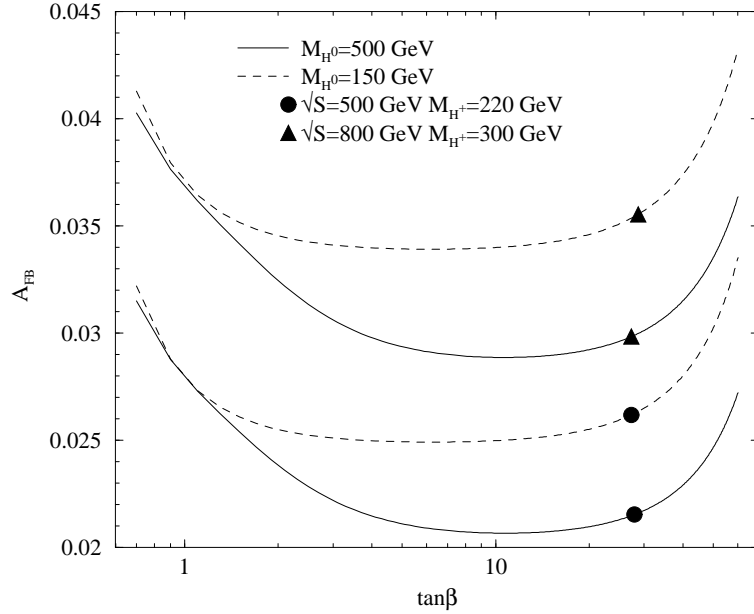
$$\Delta_{FB} = \frac{\sigma^F - \sigma^B}{\sigma^{(0)}} , \quad (4)$$

and Δ_σ is the relative correction for the integrated cross-section, see eq. (1). Formally the difference between A_{FB} and Δ_{FB} is of higher order; however, owing to the presence of large corrections to the total cross-section, it is numerically significant. Note that Δ_σ in eq. (3) should contain all the QED and weak one-loop contributions. Although the physical quantity to study is A_{FB} , the quantity Δ_{FB} can be written as the sum of the various contributions, and it is thus useful to make comparisons between the different sources of the asymmetry.

In Fig. 2 we have already presented the part of Δ_{FB} resulting from the pure photonic contributions and the asymmetry A_{FB} including only QED effects, as a function of the photon energy cut-off. The QED induced A_{FB} is rather large, reaching from $A_{FB} = 6\%$ [10%] to $\sim 1.5\%$ for set A [B]. A large part, however, is due to the large negative corrections to the integrated cross-section. The quantity Δ_{FB} is independent of this normalization effect. As can be seen in Fig. 2, the QED contributions to Δ_{FB} are between 3% [4%] for a very restrictive cut to the photon energy, and decrease to $\sim 1\%$ for a totally inclusive



(a)



(b)

Figure 6: **(a)** Weak contributions to Δ_{FB} eq. (3), and **(b)** the total forward-backward asymmetry A_{FB} for the process $e^+e^- \rightarrow H^+H^-$ in the type II 2HDM as a function of $\tan\beta$ for different values of M_{H^0} as given in the frame. The other parameters are fixed as in Fig. 3.

$\tan\beta$	M_1 [GeV]	$m_{\tilde{l}_L}$ [GeV]	$m_{\tilde{e}_R}$ [GeV]	Δ_σ [%]	Δ_{FB} [%]	A_{FB} [%]
set A: $\sqrt{S} = 500$ GeV, $M_{H^\pm} = 220$ GeV						
40	500	1000	1000	-4.160	0.874	2.728
2	1000	100	100	3.414	0.826	2.428
set B: $\sqrt{S} = 800$ GeV, $M_{H^\pm} = 300$ GeV						
40	500	1000	1000	-4.290	1.567	3.491
2	1000	100	100	2.752	1.530	3.182

Table 1: The weak corrections to the integrated cross-section (Δ_σ), the weak contributions to Δ_{FB} eq. (3), and the total forward-backward asymmetry A_{FB} for the MSSM, for given parameters. Other parameters as in Fig. 4.

treatment of the phase space. Since for a totally inclusive measurement the QED effects are largely reduced (both, in the asymmetry and the total cross-section) the purely weak effects could be accessible more easily. For definiteness we shall assume in the following discussion always the inclusive case, which corresponds to the fully integrated phase space of the radiated photon.

We now turn to the weak contributions. In the 2HDM, the quantity Δ_{FB} depends only mildly on the parameters and on the type of model. The dependence on the model parameters essentially enters through the normalization factor Δ_σ . Fig. 6 shows the part of Δ_{FB} resulting from the weak-loop diagrams (to be added to the QED one of Fig. 2) and the total forward-backward asymmetry A_{FB} , including the fully inclusive QED effects, for the general 2HDM. In Fig. 6a we see that the weak part of Δ_{FB} amounts to about 1% [1.75%] for set A [B], which is of the same order as the QED-induced part in each case (Fig 2). This means that the total forward-backward asymmetry would be largely enhanced with respect to the QED expectations. As can be seen in Fig. 6b, A_{FB} can be twice the totally inclusive asymmetry of Fig. 2; even at its minimum it is significantly larger.

The additional MSSM contributions owing to charginos and neutralinos are smaller; their effect is typically a 10% reduction of Δ_{FB} from virtual gauge and Higgs bosons. To make this more illustrative, we present in table 1 the weak-loop part of Δ_{FB} in the MSSM, and the total asymmetry A_{FB} for various sets of model parameters. The parameters used in table 1 are representative for the extreme values A_{FB} can take in the MSSM (for the given values of \sqrt{S} and M_{H^\pm}). We can see that the variation of Δ_{FB} is rather small, and the main variation of A_{FB} is again mainly due to the corrections to the normalization factor.

In general, Δ_{FB} (and so A_{FB}) as a function of S , increases with the velocity of the produced charged Higgs boson $\beta = \sqrt{1 - 4M_{H^\pm}^2/S}$.

	Δ_σ	σ [fb]	A_{FB}	N/year	$N^F - N^B/\text{year}$
QED	-18%	10	1.5%	5000	75
2HDM	-35% to -10%	8 to 11	2% to 3.4%	4000 to 5500	110 to 135

Table 2: Total corrections (Δ_σ), integrated cross-section (σ), forward-backward asymmetry (A_{FB}), number of total expected events (N) and excess of events in the forward direction ($N^F - N^B$), for the 2HDM of type II (set A: $\sqrt{S} = 500$ GeV, $M_{H^\pm} = 220$ GeV), assuming an integrated luminosity of $500 \text{ fb}^{-1}/\text{year}$.

4 Conclusions

We have presented a full $\mathcal{O}(\alpha)$ computation of the radiative corrections to the production cross-section for $\sigma(e^+e^- \rightarrow H^+H^-)$ together with a discussion for values of the charged Higgs mass relevant to the TESLA e^+e^- linear collider. The computation was done in the general framework of the type I and type II 2HDM, as well as in the MSSM.

The one-loop corrections owing to virtual gauge and Higgs particles are typically of the size $\sim 5\%$, but they can be much larger (positive) for large values of λ_5 in the general 2HDM. The ones from top and bottom quarks are negative; they can be as large as $\sim -20\%$ in the low $\tan\beta$ region, and for the type II 2HDM and the MSSM also in the region of large $\tan\beta$.

The main effect from SUSY particles to the total cross-sections originates from the squarks of the third generation, yielding large corrections provided $m_{\tilde{q}} \lesssim 500$ GeV. The chargino-neutralino contributions are of the order of a few per mille.

The forward-backward asymmetry produced by weak loop effects (Δ_{FB}) is found to be around the 1% [2%] level in the general 2HDM for set A [B]. The additional SUSY contributions to Δ_{FB} , mediated by charginos and neutralinos, are smaller, producing a decrease of 10% with respect to the 2HDM expectations.

The QED corrections from real and virtual photons are rather large: -60% to -20% [-10%] for the integrated cross-sections, and 6% [10%] to 1.5% for the asymmetries.

With the QED corrections under control it should be feasible to detect the genuine weak quantum contributions to the total cross-section. With a total inclusive measurement with respect to the photons, the QED effects can be largely diminished; in this case the QED contribution to Δ_{FB} (eq. (3)) is of the same order as the weak loop contribution. Hence, the forward-backward asymmetry is significantly increased (even doubled) compared to the QED expectations. In table 2 we present the expected number of events taking into account only the QED corrections (first line) and the complete one-loop corrections for the 2HDM case (second line), for an integrated luminosity of 500 fb^{-1} and for the parameter set A. The numbers show that the effects in the asymmetry should be detectable. On the other hand, to disentangle the effects resulting from charginos (see table 1) from the Higgs and gauge boson contributions, will require precision measurements below the 1% level.

The size of the radiative corrections depends slightly on the mass of H^+ and the energy \sqrt{S} , with similar conclusions as given above. Two examples are contained in the numerical

analysis of this article; a comprehensive description will be given in [10].

Acknowledgments

We would like to thank Thomas Hahn and Christian Schappacher for the computer-algebra-generated check. We are also thankful to Abdesslam Arhrib for numerical comparisons. This work has been partially supported by the Deutsche Forschungsgemeinschaft.

References

- [1] F. Gianotti, talk at the Vth workshop in the 2nd ECFA/DESY Study on Physics and Detectors for a Linear Electron-Positron Collider, Obernai (France) 16-19th October, 1999.
- [2] J. Gunion, H.E. Haber, G.L. Kane, S. Dawson, *The Higgs Hunter's Guide* (Addison-Wesley, Menlo-Park, 1990); *erratum* hep-ph/9302272.
- [3] H. Nilles, *Phys. Rep.* **110** (1984) 1;
H. Haber, G. Kane, *Phys. Rep.* **117** (1985) 75;
A. Lahanas, D. Nanopoulos, *Phys. Rep.* **145** (1987) 1;
See also the exhaustive reprint collection **Supersymmetry** (2 vols.), ed. S. Ferrara (North Holland/World Scientific, Singapore, 1987).
- [4] H.E. Haber, R. Hempfling, *Phys. Rev. Lett.* **66** (1991) 1815;
Y. Okada, M. Yamaguchi, T. Yanagida, *Prog. Theor. Phys.* **85** (1991) 1;
J. Ellis, G. Ridolfi, F. Zwirner, *Phys. Lett.* **B257** (1991) 83; *ibid.* **B262** (1991) 477;
R. Barbieri, M. Frigeni, *Phys. Lett.* **B258** (1991) 395;
P. Chankowski, S. Pokorski, J. Rosiek, *Nucl. Phys.* **B 423** (1994) 437;
A. Dabelstein, *Z. Phys.* **C 67** (1995) 495; *Nucl. Phys.* **B 456** (1995) 25;
J.A. Bagger, K. Matchev, D.M. Pierce, R. Zhang, *Nucl. Phys.* **B491** (1997) 3;
M. Carena, M. Quirós, C. Wagner, *Nucl. Phys.* **B 461** (1996) 407;
H. Haber, R. Hempfling, A. Hoang, *Z. Phys.* **C 75** (1997) 539;
S. Heinemeyer, W. Hollik, G. Weiglein, *Phys. Lett.* **B 440** (1998) 296; *Phys. Rev.* **D58** (1998) 091701; *Eur. Phys. J.* **C9** (1999) 343.
- [5] M. S. Alam *et al.* (CLEO Collaboration), *Phys. Rev. Lett.* **74** (1995) 2885;
J. Alexander, in *Proceedings of the 29th International Conference on High-Energy Physics*, Vancouver 1998, eds. A. Astbury, D. Axen, J. Robinson, (World Scientific, Singapore, 1999), p. 129;
S. Ahmed *et al.* (CLEO Collaboration), hep-ex/9908022.
- [6] F. Borzumati, C. Greub, *Phys. Rev.* **D58** (1998) 074004; *ibid.* **D59** (1999) 057501.

- [7] A. Kiiskinen, talk at the Vth workshop in the 2nd ECFA/DESY Study on Physics and Detectors for a Linear Electron-Positron Collider, Obernai (France) 16-19th October, 1999.
- [8] S.H. Zhu, [hep-ph/9901221](#);
A. Arhrib, C. Capdequi Peyranère, W. Hollik, G. Moulataka, in preparation.
- [9] J. Guasch, talk at the IVth workshop in the 2nd ECFA/DESY Study on Physics and Detectors for a Linear Electron-Positron Collider, Oxford 20-23 March 1999;
C. Li, B. Hu, J. Yang, *Phys. Rev.* **D47** (1993) 2865, *erratum ibid.* **D48** (1993) 3410;
J. Guasch, R.A. Jiménez, J. Solà, *Phys. Lett.* **B360** (1995) 47;
J.A. Coarasa, D. Garcia, J. Guasch, R.A. Jiménez, J. Solà, *Eur. Phys. J.* **C2** (1998) 373;
J. Guasch, J. Solà, *Phys. Lett.* **B416** (1998) 353;
J. A. Coarasa, J. Guasch, W. Hollik, J. Solà, *Phys. Lett.* **B442** (1998) 326.
- [10] J. Guasch, W. Hollik, A. Kraft, preprint KA-TP in preparation.
- [11] J. Küblbeck, M. Böhm, A. Denner, *Comput. Phys. Commun.* **60** (1990) 165;
T. Hahn, *FeynArts 2.2 user's guide*, <http://www.feynarts.de>;
T. Hahn, *FormCalc and LoopTools user's guide*,
<http://www-itp.physik.uni-karlsruhe.de/formcalc>.
- [12] A. Arhrib, M. Capdequi Peyranère, G. Moulataka, *Phys. Lett.* **B341** (1995) 313.
- [13] A. Arhrib, G. Moulataka, in Proceedings of the Workshops *Physics with e+ e- Linear Colliders* - Annecy, Gran Sasso, Hamburg, February to September 1995, Part D, ed. P.M. Zerwas, DESY 96-123D.
- [14] A. Arhrib, G. Moulataka, [hep-ph/9808317v2](#).
- [15] W. Beenaker *et. al.* in "Physics at LEP II", G. Altarelli, T. Sjöstrand, F. Zwirner editors, CERN 96-01, vol. 1, p. 79.